

# Substructure Lensing: Effects of Galaxies, Globular Clusters & Satellite Streams

D. D. Xu<sup>1,2\*</sup>, Shude Mao<sup>1</sup>, Andrew P. Cooper<sup>3</sup>, Jie Wang<sup>3</sup>, Liang Gao<sup>2,3</sup>,  
 Carlos S. Frenk<sup>3</sup>, V. Springel<sup>4,5</sup>

<sup>1</sup> Jodrell Bank Centre for Astrophysics, the University of Manchester, Alan Turing Building, Manchester M13 9PL, United Kingdom

<sup>2</sup> National Astronomical Observatories, Chinese Academy of Sciences, Beijing, 100012, China

<sup>3</sup> Institute for Computational Cosmology, Dept. of Physics, University of Durham, South Road, Durham DH1 3LE, United Kingdom

<sup>4</sup> Max-Planck Institut Für Astrophysik, Karl-Schwarzschild-Straße 1, 85740 Garching, Germany

<sup>5</sup> Heidelberg Institute for Theoretical Studies, University of Heidelberg, Schloss-Wolfsbrunnengweg 35, D-69118 Heidelberg, Germany

Accepted ..... Received ..... ; in original form.....

## ABSTRACT

Lensing flux-ratio anomalies have been frequently observed and taken as evidence for the presence of abundant dark matter substructures in lensing galaxies, as predicted by the cold dark matter (CDM) model of cosmogony. In previous work, we examined the cusp-caustic relations of the multiple images of background quasars lensed by galaxy-scale dark matter haloes, using a suite of high-resolution  $N$ -body simulations (the Aquarius simulations). In this work, we extend our previous calculations to incorporate both the baryonic and diffuse dark components in lensing haloes. We include in each lensing simulation: (1) a satellite galaxy population derived from a semi-analytic model applied to the Aquarius haloes, (2) an empirical Milky-Way globular cluster population and (3) satellite streams (diffuse dark component) identified in the simulations. Accounting for these extra components, we confirm our earlier conclusion that the abundance of intrinsic substructures (dark or bright, bound or diffuse) is not sufficient to explain the observed frequency of cusp-caustic violations in the CLASS survey. We conclude that the observed effect could be the result of the small number statistics of CLASS, or intergalactic haloes along the line of sight acting as additional sources of lensing flux anomalies. Another possibility is that this discrepancy signals a failure of the CDM model.

**Key words:** Gravitational lensing - dark matter - galaxies: ellipticals - galaxies: formation

## 1 INTRODUCTION

The cold dark matter (CDM) cosmogony predicts that cosmic structures form hierarchically through a succession of mergers and accretions. The mass of the Milky Way’s own dark halo is currently constrained to  $\sim 1 - 5 \times 10^{12} M_{\odot}$  (e.g. Guo et al. 2009). Numerical simulations predict a wealth of dark matter substructures (self-bound subhaloes) surviving in haloes of this mass (e.g. Gao et al. 2004; Gao et al. 2004; Diemand et al. 2008; Springel et al. 2008). These substructures have a power-law mass function; scaling this to a satellite galaxy luminosity function (LF) by adopting a fixed mass-to-light ratio consistent with the brightest objects overpredicts the number of satellite galaxies of the Milky Way (MW) and M31 by a factor of several hundred – the so-called ‘missing satellite’ problem (e.g. Klypin et al. 1999;

Moore et al. 1999; for a recent review see Kravtsov 2010). For many years, theoretical models of galaxy formation have predicted that the star formation efficiency in low-mass haloes can be strongly suppressed through a combination of photoionization (Efsthathiou 1992) and supernova feedback (White & Rees 1978). This suppression renders many such haloes permanently ‘dark’ and may solve the apparent discrepancy (e.g. Kauffmann et al. 1993; Bullock et al. 2000; Gnedin 2000; Benson et al. 2002; Okamoto & Frenk 2009; Macciò et al. 2009; Li et al. 2010; Stringer et al. 2009). Recent discoveries of low luminosity satellites in the MW and M31 and corrections for incompleteness (e.g. Koposov et al. 2008; Tollerud et al. 2008) imply reasonable agreement between observations and theoretical predictions for MW-like haloes (Benson et al. 2002). However, because they rely on uncertain baryonic physics and currently limited data, these comparisons so far only provide an indirect and uncertain test of the abundance and mass function of CDM substructure.

\* E-mail: dandanxu@jb.man.ac.uk; dandanxu@bao.ac.cn

tures. Since gravitational lensing traces mass, regardless of its luminosity, it can provide a powerful alternative tool to investigate otherwise ‘hidden’ subhaloes and directly test the CDM model (e.g. MacLeod et al. 2009; Vegetti et al. 2009).

Flux-ratio anomalies observed in multiple images of lensed quasars are often cited as evidence for substructures in lensing galaxies (e.g. Mao & Schneider 1998; Metcalf & Madau 2001; Metcalf & Zhao 2002; Dalal & Kochanek 2002; Chiba 2002; Kochanek & Dalal 2004; Metcalf et al. 2004; Chiba et al. 2005; Sugai et al. 2007; McKean et al. 2007; More et al. 2009). Some studies, e.g. Dalal & Kochanek (2002), Bradač et al. (2004) using CDM simulations have concluded that the substructure population expected for a galaxy-scale lens can reproduce the observed flux anomaly cases. However, other studies, e.g. Mao et al. (2004), Amara et al. (2006), Macciò et al. (2006), Macciò & Miranda (2006) and our own previous work (Xu et al. 2009) have argued that the simulated CDM substructure population is *not* sufficient to explain the observed frequency of lensing flux-ratio anomalies. This negative conclusion does not yet rule out the predictions of CDM, as the observed sample of ‘anomalous’ lenses is small. Intergalactic haloes along the line of sight may also perturb the lensing potential and cause the observed lensing anomalies (Chen et al. 2003; Wambsganss et al. 2005; Metcalf 2005a,b; Miranda & Macciò 2007; Puchwein & Hilbert 2009).

One extreme case of flux-ratio anomalies is the cusp-caustic violation, which has been observed in five lens systems of a cusp geometry: B0712+472 (Jackson et al. 2000, 1998), B1422+231 (Impey et al. 1996; Patnaik & Narasimha 2001), B2045+265 (Fassnacht et al. 1999), RXJ1131-1231 (Sluse et al. 2003) and RXJ0911+0551 (Bade et al. 1997; Burud et al. 1998). In the first three cases (those detected in radio observations) these have been attributed to substructure lensing, while the remaining two are thought to be due to microlensing (Anguita et al. 2008; Morgan et al. 2006). In Xu et al. (2009) (which we summarise below) we found that even with the well-resolved subhalo population from the Aquarius simulations, the observed cusp lenses still violate the cusp-caustic relation more frequently than expected for a concordance CDM model. However, our earlier work did not consider the effect of baryons concentrated at the centre of subhaloes, which may modify their density profiles and so alter their lensing properties. In this work, we carry out a more thorough analysis of the lensing effect of baryons in substructures, proceeding as follows. In Section 2 we use a semi-analytic model of galaxy formation to predict the baryon content of subhaloes in each Aquarius simulation: we model the density distribution of baryons in each subhalo and re-run our lensing simulations to study cusp-caustic violations. In Section 3, to estimate the effects of possible baryonic concentrations below the resolution limit of the simulation, we further include an empirical Galactic globular cluster population (Harris 1996) in our model. Finally, as typical surface density fluctuations of only a few per cent would be sufficient to cause flux-ratio anomalies (Mao & Schneider 1998; Li et al. 2006), we consider irregularities in the surface density of the main halo due to the debris of tidally disrupted satellites (the

diffuse component) in Section 4. Section 5 provides a short summary and a brief discussion of our results.

## 2 SEMI-ANALYTIC GALAXIES AND THEIR CUSP-CAUSTIC VIOLATIONS

### 2.1 The Aquarius Simulations

The Aquarius project (Springel et al. 2008; Springel et al. 2008) is a suite of collisionless  $\Lambda$ CDM  $N$ -body simulations run with the GADGET-3 code. Each of the six simulations in the suite (labelled A-F) centres on a single halo of mass  $\sim 10^{12}h^{-1}M_{\odot}$ . These haloes were selected for high-resolution multi-mass resimulation from a  $100h^{-1}\text{Mpc}^3$  simulation with a uniform mass resolution: a subsequent high-resolution study of this parent volume (the Millennium II simulation) confirms that in almost all respects the Aquarius sample is representative of haloes of this mass (Boylan-Kolchin et al. 2009; Boylan-Kolchin et al. 2009).

All six haloes were simulated at a resolution corresponding to a particle mass of  $\sim 10^4h^{-1}M_{\odot}$  and a softening length of  $\sim 50h^{-1}\text{pc}$ , resulting in  $\sim 130$  million particles within the virial radius of the main halo at  $z = 0$ . This resolution of the Aquarius project is referred to as ‘level 2’ and the six haloes at this resolution are labelled *Aq-A-2*, *Aq-B-2*, *Aq-C-2*, *Aq-D-2*, *Aq-E-2* and *Aq-F-2*. At this resolution, subhaloes are resolved to a mass limit of  $m_{\text{sub}} \gtrsim 10^5h^{-1}M_{\odot}$  (corresponding to bound associations of 20 particles identified by the SUBFIND algorithm). We use these level 2 simulations in this work. Simulations of one halo (Aq-A) at higher and lower resolutions have demonstrated that the abundance, radial distribution and internal structure of subhaloes relevant to our lensing calculations are numerically converged to high accuracy at the resolution of the level 2 simulations (full details of these extensive convergence studies are given by Springel et al. (2008) and Navarro et al. (2010)).

Throughout this work, the cosmology of our lensing simulations is the same as that used for the Aquarius project, with a matter density  $\Omega_{\text{m}} = 0.25$ , cosmological constant  $\Omega_{\Lambda} = 0.75$ , Hubble constant  $h = H_0/(100\text{km s}^{-1}\text{Mpc}^{-1}) = 0.73$  and linear fluctuation amplitude  $\sigma_8 = 0.9$ .

### 2.2 Halo lensing model

In Xu et al. (2009), we studied cusp-caustic violation probabilities using the six galaxy-scale CDM haloes provided by the Aquarius simulations. Mock lensing signals from background quasars were used to determine the observed frequency of flux-ratio anomalies due to dark matter substructures in these haloes. The mass resolution of Aquarius is at least two orders of magnitude higher than that of previous simulations used for lensing studies, resolving bound subhaloes down to a mass of  $\sim 10^5h^{-1}M_{\odot}$ . In addition to the simulated dark matter distribution, we added a Hernquist profile ‘galaxy’ at the centre of each main halo. We renormalized the dark matter particle mass and adiabatically contracted the particle distribution to account for this extra contribution to the potential (e.g. Barnes & White 1984; Blumenthal et al. 1986; Mo et al. 1998; Gnedin et al. 2004).

A particle-mesh (PM) code was applied to calculate

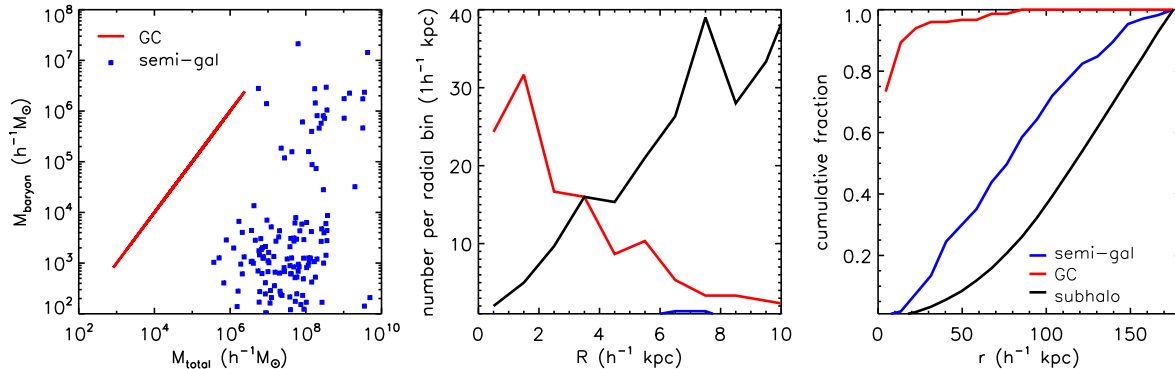


**Figure 1.** The masses and radial distributions of semi-analytic galaxies (blue) and dark matter subhaloes (black) from *Aq-A-2*, as well as the observed Milky-Way globular clusters (red; using the catalogue from Harris 1996). The panel on the left shows the stellar mass  $M_{\text{baryon}}$  as a function of the total mass  $M_{\text{total}}$ , which in the case of semi-analytic galaxies is the total mass of a satellite galaxy and its host subhalo. The dynamical masses of globular clusters come from their observed V-band luminosities, assuming a mass-to-light ratio to be 3. Such masses are equal to their stellar masses  $M_{\text{baryon}}$ , assuming a zero dark matter content. In general, globular clusters have lower dynamical masses than satellite galaxies, but the latter have higher mass-to-light ratios than the former. The middle and right panels present the projected and 3D radial distributions of the three components. Globular clusters are much more concentrated towards the galactic centre than satellite galaxies. At the Einstein radius of the main halo ( $2 \sim 4h^{-1}$  kpc), the number of projected globular clusters is about 1  $\sim$  2 times that of dark matter subhaloes. Satellite galaxies are rare in the projected central region.

lensing potentials, deflection angles and magnifications from the simulated lensing haloes. The numerical accuracy of this code is described fully in Xu et al. (2009). Near the critical curves, high magnification makes changes in the image properties sensitive to small perturbations in surface density. To estimate the effects of numerical noise in these regions, we used our code to calculate the lensing properties of isothermal ellipsoids generated by Monte Carlo sampling, using an equivalent number of particles to the level 2 Aquarius simulations ( $\sim 10^8$  particles within the radius  $r_{200}^1$ ). The numerical accuracy of the deflection angle, convergence (surface density) and magnification for these Monte Carlo realisations are shown in Figure 4 of Xu et al. (2009). The uncertainties around the Einstein radius (at about  $0.02 r_{200}$ ) are 0.2% for the deflection angle, 1% for the convergence, and  $< 10\%$  for the magnification. Figure 6 of Xu et al. (2009) presents the probability distribution function of the image flux ratio  $R_{\text{cusp}}$  (Eq. 1) for cusp sources with an image opening angle smaller than  $90^\circ$  in the  $10^8$ -particle Monte Carlo realisations. This distribution was found to be broader than the equivalent analytical calculation as the result of discreteness noise, inherent in mapping an  $N$ -body density field to a mesh.

To correct for this sampling noise, each main Aquarius halo (including a central ‘galaxy’) was modelled as an isothermal ellipsoid (e.g. Rusin et al. 2003; Rusin & Kochanek 2005; Koopmans et al. 2006; Gavazzi et al. 2007), the lensing properties of which can be solved analytically. These ellipsoids were determined as best fits to the critical curves and caustics of the main galaxy haloes. The substructure population of each halo was taken directly from the simulations and superimposed on the analytic density fields of these isothermal ellipsoids. Multiple images of mock background quasars were recov-

ered through an image-finding procedure combining the Newton-Raphson and Triangulation methods (for a more detailed description of this procedure, see Xu et al. (2009)). The cusp-caustic relations and their violation probabilities were calculated for the simulated lensing-galaxy haloes and compared to those derived from observations. In this paper we extend this method to study additional contributions to the lensing potential.

### 2.3 Semi-analytic galaxies

The Aquarius simulations provide us with particle distributions of the main dark matter haloes and an associated population of subhaloes. To investigate the effect of baryons in substructures, we postprocess Aquarius with the GALFORM semi-analytic model (Cole et al. 1994, 2000; Bower et al. 2006). We determine the dark matter merger history of each subhalo directly from the simulations (Helly et al. 2003). From each of these ‘merger trees’, GALFORM computes the history of gas accretion, star formation and feedback in the corresponding galaxy. Here, as a fiducial model, we adopt the parameter values of Bower et al. (2006), which have been shown to be consistent with a number of observational constraints. As discussed by Cooper et al. (2010), the Bower et al. (2006) parameters also agree well with the MW and M31 satellite galaxy LFs, provided that the value of the parameter  $V_{\text{cut}}$  is set to  $\sim 30 \text{ km s}^{-1}$  (a value consistent with recent estimates from numerical simulations<sup>2</sup>), in preference to the value of  $50 \text{ km s}^{-1}$  used by Bower et al. (2006). A discrepancy with observations is only apparent at  $M_V \gtrsim -5$ , where constraints on the observed LF are weak. We stress that GALFORM is only used here to determine which dark

<sup>1</sup> Defined as the radius enclosing a mean density of 200 times the critical density of the Universe.

<sup>2</sup>  $V_{\text{cut}}$  is defined as the halo circular velocity below which a photoionizing background strongly suppresses further baryon accretion and cooling. Reionization is assumed to occur instantaneously at  $z = 6$  in the Bower et al. (2006) model.

matter substructures host stars, and to assign reasonable mass-to-light ratios to those substructures. For this purpose, a fiducial model producing a satellite LF consistent with the available data is sufficient. Our choice of the Bower et al. (2006) parameters with  $V_{\text{cut}} = 30 \text{ km s}^{-1}$  is identical to that used by Cooper et al. (2010) as a fiducial model in their study of galactic stellar haloes. Our findings concerning the lensing effect of substructures are not strongly sensitive to further changes in this model that could be made to match other properties of the satellite population.

Populating the resolved subhaloes of Aquarius with our fiducial GALFORM model results in  $\sim 100 - 200$  satellite galaxies within the virial radius of each Aquarius halo. As an example, Fig. 1 presents the properties of the semi-analytic galaxies (shown as blue symbols) in the halo *Aq-A-2*. The combined mass,  $M_{\text{total}}$ , of a satellite galaxy and its host subhalo ranges from  $\sim 10^6 h^{-1} M_{\odot}$  to  $\sim 10^{10} h^{-1} M_{\odot}$  with a median of  $\sim 3 \times 10^7 h^{-1} M_{\odot}$ . The baryonic mass  $M_{\text{baryon}}$  spans more than six decades, which is consistent with the wide range of MW satellite luminosities (from  $\sim 100 L_{\odot}$  to  $\sim 10^8 L_{\odot}$ , e.g. Strigari et al. 2008; Koposov et al. 2008; Stringer et al. 2009). Their radial distribution has a median halo-centric distance of  $70 h^{-1} \text{ kpc}$ . It is rare to find a satellite galaxy projected within the Einstein radius of the main halo ( $2 \sim 4 h^{-1} \text{ kpc}$ ).

We require a structural model for each satellite galaxy in its host subhalo. Although GALFORM predicts the morphology and size of each simulated galaxy, we prefer to adopt a simpler and more conservative model that *maximises* the lensing effect. We describe all satellite galaxies using a singular isothermal sphere (SIS) density profile. This profile, of the form  $\rho(r) \propto r^{-2}$ , leads to a constant deflection angle. The SIS profile of each galaxy terminates at a radius  $r_t$ , which we set to be the half-mass radius  $r_H$  of the galaxy’s host dark matter subhalo (resulting in a median truncation radius of  $\sim 200 h^{-1} \text{ pc}$ ). The total stellar mass of the galaxy predicted by GALFORM is enclosed within  $r_t$ . Under these assumptions, the median Einstein radius is  $\sim 0.006''$ . Further increasing the concentration of our stellar components by setting  $r_t = 0.3 r_H$  (median  $r_t \sim 60 h^{-1} \text{ pc}$ ) makes little difference to the final cusp-caustic violation probability (as discussed below, this is sensitive to the spatial distribution of the substructures in the main halo - see Fig. 1). All satellites have high mass-to-light ratios such that adiabatic contraction due to the baryonic component can be neglected. The full hierarchy of sub-subhaloes within subhaloes is included in the lensing calculation, as in our earlier dark matter-only study. Galaxies hosted by these sub-subhaloes are also represented by SIS profiles in this updated calculation.

To determine the new cusp-caustic violations that result from including baryons in dark substructures, the semi-analytic galaxies are added to the dark matter density fields from Aquarius. For the dark matter component of each subhalo, the particle distribution from the simulation is used directly, as in our earlier study; we only assume SIS profiles for the stars. The new density fields are processed through our PM code and the image-finding routine to recreate lensing signals of background quasars.

## 2.4 The cusp-caustic violation

In any smooth lensing potential an asymptotic magnification relation (the ‘cusp-caustic relation’; Blandford & Narayan 1986; Schneider & Weiss 1992; Zakharov 1995; Keeton et al. 2003) will hold:

$$R_{\text{cusp}} \equiv \frac{|\mu_A + \mu_B + \mu_C|}{|\mu_A| + |\mu_B| + |\mu_C|} \rightarrow 0, \quad (1)$$

where  $\mu$  denotes the magnifications of the three closest images *A*, *B* and *C* of a background source, which is located near a cusp of the central caustic. In this case, the total absolute magnification  $|\mu_A| + |\mu_B| + |\mu_C|$  of the triple images goes to infinity. Following the same procedure as Xu et al. (2009), the lensing haloes are located at redshift 0.6 and the background quasars at redshift 3.0. ‘Cusp sources’ are defined as sources (quasars) that are near the cusps of the central caustic and have image opening angles,  $\Delta\theta$  of their close triple images smaller than  $90^\circ$ . Any cusp source with  $R_{\text{cusp}} \geq 0.187$  is defined as a cusp-violation case, as 0.187 is the observed value for B1422+231, which shows the smallest violation (smallest  $R_{\text{cusp}}$  value) among the five observed cusp lenses. In each of the three independent projections from each Aquarius halo, approximately 10000 - 20000 cusp sources are generated and used to calculate the  $R_{\text{cusp}}$  distribution and the violation probability.

Our earlier work (Xu et al. 2009) found an average cusp-violation rate of  $\sim 10\%$  over all three independent projections of each of the six haloes<sup>3</sup>, which leads to a probability  $< 0.01$  of observing 3 out of 5 cusp lenses violating the cusp-caustic relation due to substructures. This result is listed as case (a) in Table 1, which summarises the effects of additional contributions to the lensing potential.

Case (b) in Table 1 adds the semi-analytic galaxies described above to the dark matter substructures. The change in the cusp-caustic violation is small. The reason for this is clear from Fig. 2 (left), which shows the critical curves superimposed on a contour map of the substructure surface mass fraction, in the halo *Aq-E-2* (a single projection is shown as an example; our results are averaged over many projections). This figure can be compared with figure 11 in Xu et al. (2009): the addition of satellite galaxies alters the density profile of individual subhaloes, but cannot alter the abundance of substructures around the tangential critical curve, where the cusp-caustic relation is examined. Therefore, the baryonic ‘boost’ from the small number of galaxy-hosting subhaloes contributing to the overall cusp-caustic violations is marginal.

As shown in Table 3 of Xu et al. (2009), the violation probability varies from halo to halo, and from projection to projection within the same halo. The lensing cross-section for cusp-caustic violation is significant only where massive substructures are projected onto the central region. The presence or absence of these strong perturbations to the lensing potential is highly stochastic, because massive subhaloes

<sup>3</sup> There were four projections in total with naked cusps (see Xu et al. 2009) present in the central caustic due to the large core sizes of the imposed Hernquist profiles. The exclusion of these four cases in the final calculation resulted in a mean cusp-violation rate of 6.4%. Here in order to avoid these “naked cusps”, the core size is artificially set to be  $0.05''$  for all six haloes, leading to the higher cusp-violation rate of  $\sim 10\%$  as shown in Table 1 case (a).

**Table 1.** The average substructure surface mass fractions and the cusp-caustic violation probabilities for scenarios in which additional contributions to the lensing potential are considered. Col. 2:  $f_{\text{sub,annu}}$  is the mean surface mass fraction of substructures within an  $0.1''$ -annulus around the tangential critical curve. Col. 3:  $P(R_{\text{cusp}} \geq 0.187)$  is the mean cusp-violation rate averaged over all projections from six haloes, under which Col. 4,  $P_{3|5}$ , gives the probability of observing 3 out of 5 cusp lenses violating the cusp-caustic relation due to the presence of substructures.

Case	$f_{\text{sub,annu}}$	$P(R_{\text{cusp}} \geq 0.187)$	$P_{3 5}$
(a), dark matter subhaloes only	0.20%	10.1%	0.8%
(b), (a) + semi-analytic galaxies	0.21%	10.2%	0.9%
(c), (b) + Milky-Way globular clusters	0.23%	11.0%	1.1%

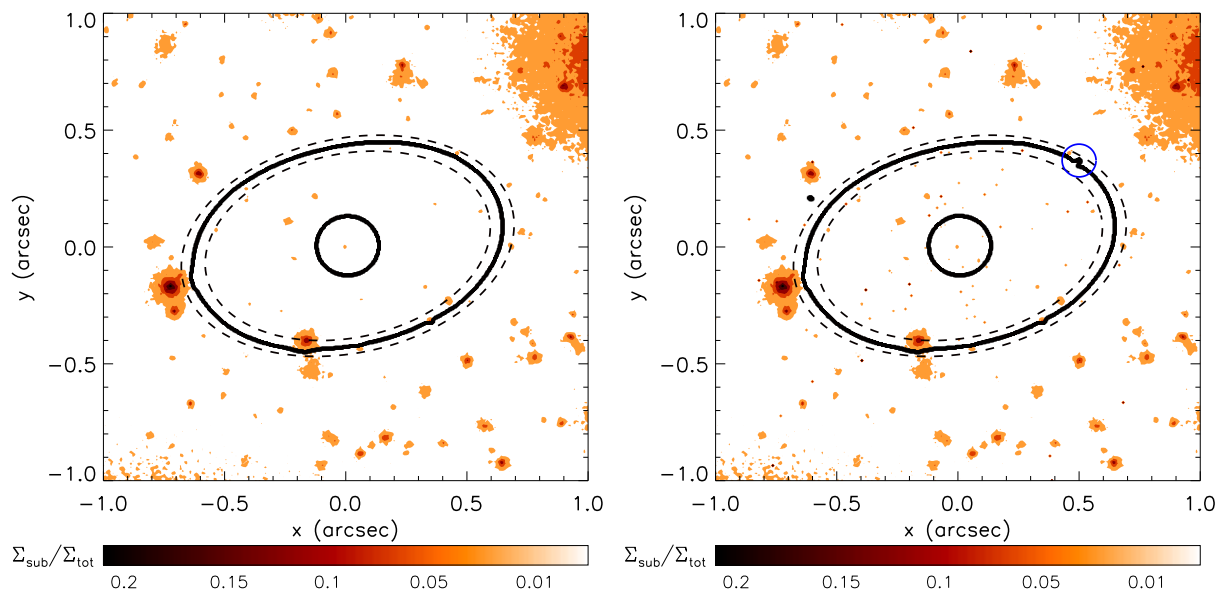


**Figure 2.** Contour maps of the substructure surface mass fraction of the halo *Aq-E-2*, in *X*-projection. Left: semi-analytic galaxies are added to the dark matter subhalo population. The mean surface mass fraction,  $f_{\text{sub,annu}}$  of the substructures within the  $0.1''$ -annulus (indicated by the dashed lines) around the tangential critical curve is  $\sim 0.16\%$ . Right: semi-analytic galaxies and Milky-Way globular clusters are added to the dark subhalo population.  $f_{\text{sub,annu}} \sim 0.19\%$ . Globular clusters are more centrally distributed in the projected central region than satellite galaxies. The blue circle indicates an example of the small-scale wiggles induced by globular clusters.

are intrinsically rare and are typically found in the outer regions of their hosts. It is therefore possible in principle that a limited sample of haloes and projections could lead to an underestimate (or overestimate) of the violation probability. However, the mass function and radial distribution of subhaloes is found to be very similar among all six Aquarius haloes (Springel et al. 2008). In these respects the Aquarius haloes are themselves representative of the population from which they were selected (Boylan-Kolchin et al. 2009). Our sample of 18 projections (combining three projections in six similar haloes) is therefore unlikely to significantly underestimate the violation probability.

### 3 MILKY-WAY GLOBULAR CLUSTERS AND THEIR CUSP-CAUSTIC VIOLATIONS

Scenarios for the formation of globular clusters (GCs) are numerous and highly uncertain. GCs are known to have low mass-to-light ratios (i.e. to be baryon-dominated) at the present day (e.g. Maraston 2005), although a past associa-

tion between individual GCs and dark matter haloes is not strongly ruled out. It may be that some GCs are the relics of the very first generations of star formation in the early Universe (e.g. Gao et al. 2009; Griffen et al. 2009). It is often speculated that a number of GCs (most notably  $\omega$  Centauri) should be identified with the stripped nuclei of dwarf satellite galaxies. This suggests that the definitions of these two classes of object might be ambiguous. At the present day GCs are strongly concentrated around central galaxies (more so than the overall subhalo populations in simulated CDM haloes) and their survival is known to be subject to many factors, including evaporation and tidal disruption. GCs are likely to be present in lensing galaxies in large numbers and may perturb the gravitational potentials in the inner regions, causing cusp-caustic violations. A simple estimate of their contribution was made by Mao & Schneider (1998), who concluded that a surface density fluctuation of a few per cent ( $\delta\kappa \sim 0.01$ ) from GCs would be enough to cause the observed flux-ratio anomaly in B1422+231. This conclusion has been re-examined in this work.

Here we adopt an empirical approach to the effects of GCs on the lensing potential. We use the catalogue of Milky-Way GCs from Harris (1996), which provides their spatial distribution, V-band luminosities  $L_V$  and half-mass radii  $r_h$ . Although the Milky-Way GC distribution is slightly flattened within the central  $\sim 10h^{-1}$  kpc, the choice of projection does not affect our results.

It is interesting to ask whether a proportion of the ‘satellite galaxies’ in Aquarius should in fact be identified with a population of ‘primordial’ galaxy-like objects or with the ‘cores’ of galaxies that have been heavily stripped. We have already included satellites in our calculation, so our approach to GCs risks double-counting some objects if either of these cases is true. However, a detailed investigation of this issue is beyond the scope of this paper, and we will assume that most GCs are not already represented as ‘satellites’ in our semi-analytic model. As we state above, the LF of bright satellite galaxies in our model matches the shape of the Milky-Way satellite LF. This observed LF does not include the many equally bright but structurally distinct Milky-Way GCs: this in turn suggests that these bright GCs are not represented by some of the existing ‘satellites’ in our model, stripped or otherwise. Fainter than  $M_V \sim -5$  the distinction between galaxies and clusters is much less certain and the interpretation of the current data is not at all clear. However, these low-mass objects are not significant for lensing.

The masses of our empirical Milky-Way GCs are obtained assuming  $M/L_V = 3$  (e.g. Maraston 2005). We adopt a SIS profile for each GC to maximise our estimate of its lensing effect. We choose the SIS truncation radius  $r_t = 2r_h$  such that the model half-mass radius is equal to the GC half-light radius ( $M_{\text{SIS}}(< r) \propto r$ ). The median Einstein radius is  $\sim 0.003''$  under these assumptions. Fig. 1 summarises our empirical GC population, showing the masses and radial distributions of the Milky-Way GCs (red symbols). Their dynamical masses range from hundreds to millions of solar masses (lower than that of the majority of satellite galaxies). The radial distribution of GCs is much more concentrated than satellite galaxies: the number of GCs projected at the Einstein radius of the main halo is about  $1 \sim 2$  times the number of the dark matter subhaloes at that radius.

Comparing the right and left panels in Fig. 2, more substructures (GCs) in this case are projected in the vicinity of the tangential critical curves, inducing more smaller-scale wiggles; one example is indicated by the blue circle. Case (c) in Table 1 summarises our lensing results after including the empirical GC population. The mean cusp-violation rate averaged over all projections from six Aquarius haloes has only marginally increased from  $\sim 10\%$  to  $\sim 11\%$ , and the probability to observe 3 out of 5 cusp lenses violating the cusp-caustic relation due to substructures has increased from 0.9% to 1.1%. Although GCs are numerous and more concentrated than the subhalo population, the small mass and size of a typical GC limits their effect on the lensing potential. The predicted violation rate is still far below that observed, so the inclusion of GCs still does not solve the apparent lack of substructures suggested by observations of lensing flux anomalies.

#### 4 AQUARIUS STREAMS AND THEIR CUSP-CAUSTIC VIOLATIONS

In recent years, streams and other stellar overdensities have been detected in the halo of the Milky Way (e.g. Belokurov et al. 2007; Belokurov et al. 2007) and other nearby galaxies, most notably M31 (e.g. McConnachie et al. 2009). Cosmological  $N$ -body simulations have demonstrated that a wealth of similar structures consistent with these observations are produced by the tidal stripping of satellite galaxies in typical Galactic haloes (e.g. Helmi & White 1999; Cooper et al. 2010). As stars in satellites are likely to be deeply embedded in their own host dark matter (sub)haloes at the time of accretion, each stellar stream in these models is naturally associated with a more massive stream of dark matter. These ‘streams’ exhibit a variety of complex morphologies (e.g. Cooper et al. 2009), very few of which remain ‘coherent’ in configuration space for long. However, their presence might induce irregularities in the surface density of the dark matter halo and cause lensing flux anomalies.

We make an estimate of the magnitude of this effect with the level-2 Aquarius simulations. We define streams as dark matter particles that were once bound to substructures crossing the virial radius of the main halo, but which at  $z = 0$  are bound to the main halo itself (i.e. are no longer bound to any substructure). In the previous sections and in Xu et al. (2009), all these particles were treated as the smooth component of the main halo (included in the smooth ellipsoidal fit). The streams from different infalling substructures are phase-mixed to different degrees. Those most strongly mixed are smoothly distributed as ellipsoids concentric with the main halo, but a small quantity of satellite (dark matter) debris remains in the form of coherent features in configuration space (canonical ‘streams’). These features introduce the most significant surface density irregularities.

Here we select the most massive spatially coherent streams that are projected within the central  $\sim 10h^{-1}$  kpc region of each halo. We do so by visually inspecting the density fields of all massive streams ( $M_{\text{DM}} > 5 \times 10^8 h^{-1} M_\odot$ ) for regions of high overdensity projected in the vicinity of the critical curve. We have calculated the lensing effect of each individual candidate stream by superimposing its full particle distribution onto our smooth isothermal ellipsoid model for the main halo, as we did for the bound substructures described previously. In practice the overlap of many such streams at the centre of a lensing galaxy decreases the density contrast of any single stream; by isolating these streams from the smoothly distributed dark matter, we are likely to *overestimate* their overall contribution.

Fig. 3 shows one example of the massive coherent streams meeting our criteria. The surface density contours are overlaid by the lensing critical curves. The mean surface mass fraction,  $f_{\text{stm,annu}}$ , of the stream within the  $0.1''$ -annulus around the tangential critical curve, varies from 0.01% to  $< 1\%$  depending on projection. The cusp-violation rates in all cases are found to be extremely low,  $P(R_{\text{cusp}} \geq 0.187) \ll 1\%$ , even for projections with  $f_{\text{stm,annu}}$  as high as those from compact substructures. The typical width of these ‘dense’ spatially coherent streams is of the order of  $\sim \text{kpc}$  (e.g. Helmi & White 1999): this is about the size of

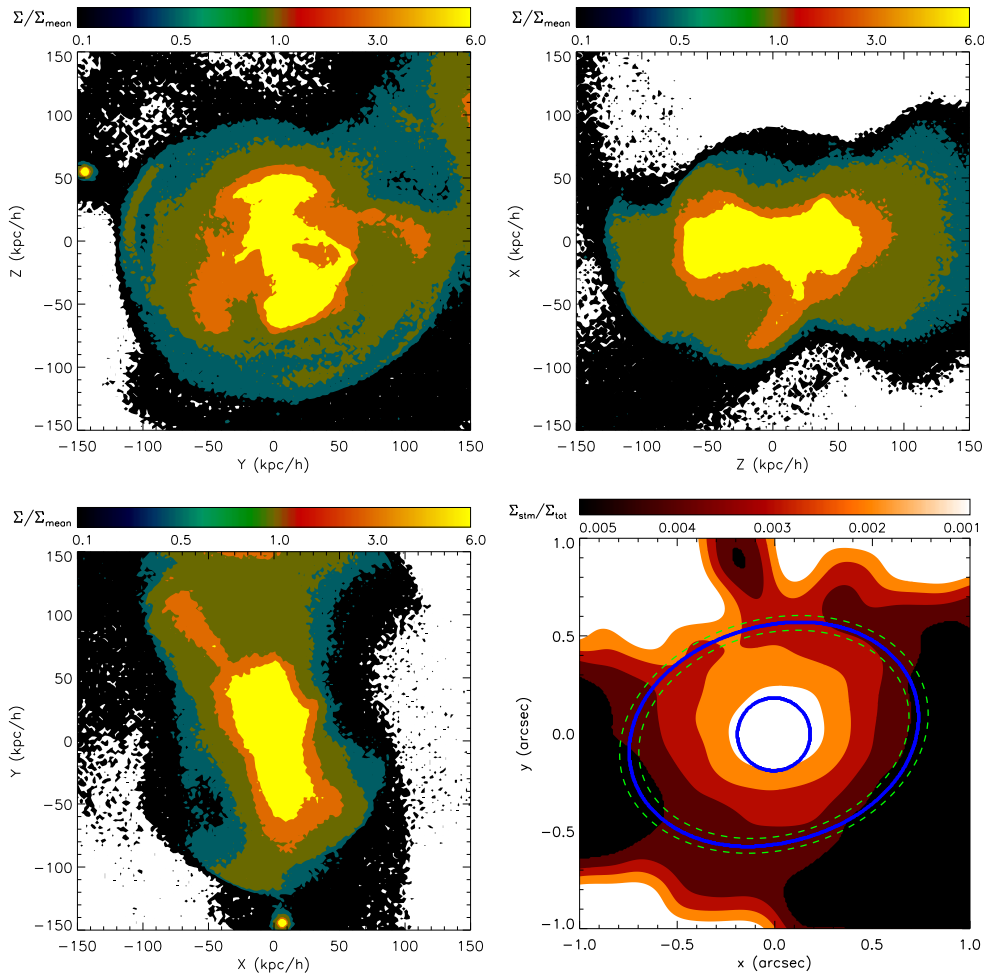


**Figure 3.** An example of one spatially coherent stream in the halo *Aq-A-2*. The top two and bottom left panels show the stream on large scales in three independent projections. The bottom right panel presents the contour map of the surface mass density fraction of the stream on smaller scales in *Y*-projection, with critical curves overlaid;  $f_{\text{stm,annu}} \sim 0.45\%$ .

the strong lensing domain and hence these streams are incapable of inducing small-scale wiggles in the tangential critical curves. On the other hand, thin streams from lower mass progenitors are not sufficiently dense. We conclude that the presence of dark matter streams does not significantly boost the cusp-caustic violations.

## 5 DISCUSSION AND CONCLUSIONS

We briefly discuss a few issues which may affect our conclusions. Firstly, the observed sample is small, consisting of only five cusp lenses, among which are the three systems detected in the radio band by the CLASS survey (Myers et al. 2003; Browne et al. 2003). This survey shows an anomalously high incidence of secondary lenses (bright satellites) (Bryan et al. 2008; Jackson et al. 2010).

A larger sample of galaxy-scale lenses from future instruments will provide better statistical constraints on substructure abundance in galaxy-sized CDM haloes (Vegetti & Koopmans 2009). New lenses are likely to be discovered in optical surveys (such as PanSTARRS and LSST), although radio and mid-infrared follow-up will be

necessary to distinguish anomalies attributable to substructure from microlensing events (e.g. Wambsganss et al. 1990; Witt et al. 1995; Pooley et al. 2007; Eigenbrod et al. 2008). High-resolution radio surveys (to be carried out by LOFAR and SKA, for example) will be a productive way to discover more of these systems.

Secondly, most lensing galaxies are massive elliptical galaxies due to their large lensing cross-sections (Turner et al. 1984). Compared with their spiral and irregular counterparts, massive ellipticals are known to host more GCs (e.g. Forte et al. 1982; Harris 1991, 1993; West 1993). In this work, we consider the lensing effect of GCs by imposing the observed Milky-Way GC population. If the lens galaxies are much more massive than the Aquarius haloes, this assumption may underestimate the appropriate GC abundance. However, even with an increased number of GCs typical of massive ellipticals, we would not expect major changes to our conclusions.

Thirdly, the semi-analytic galaxies that we have included in the lensing simulation are all hosted by dark matter subhaloes above the resolution limit of the Aquarius simulations. However, semi-analytic models also follow the at-

tached stellar components even after their host dark matter (sub)haloes are tidally stripped below 20 particles ( $\sim 10^5 h^{-1} M_\odot$ ). The baryonic masses of these ‘sub-resolution’ stellar components are in the same range as those of satellite galaxies, and each is associated with a bound dark structure no more massive than  $10^5 h^{-1} M_\odot$ . In GALFORM their survival depends on an estimate of their merger timescales, which is subject to the treatment of dynamical friction. The radial distribution of the centres (most-bound particles) of these objects is more concentrated than that of their counterparts with resolved dark haloes. Nevertheless, including these sub-resolution ‘orphan galaxies’ only marginally increases the cusp-violation probability under the assumption of singular isothermal spheres for their density profiles.

Finally, when including semi-analytic galaxies to account for the lensing effect of baryonic substructures, we have assumed that the overall galactic potential and the dynamics of subhaloes would not be significantly modified if baryons were added to our dark matter-only simulations. However, a concentration of baryons at the centre of a subhalo may increase its resilience to tidal stripping. The abundance of subhaloes in the inner region of the main halo may increase as a result of this effect. Our model does not account for this ‘baryon-enhanced’ survival of a small number of massive objects, although we do not consider this omission to be significant. There are likely to be few such objects, as a subhalo must typically lose more than  $\sim 90\%$  of its mass before the structure of its central (stellar) core influences further stripping (see e.g. Peñarrubia et al. 2008). This naturally limits the number of ‘marginally destroyed’ cases that would change in a fully self-consistent model. Another effect of including baryons would be to increase the concentration of the main halo in our simulation, resulting in a stronger tidal field. However, studies of disc-subhalo interactions using the Aquarius haloes (Lowing et al. in prep) support our assumption that the subhalo population (in the regime relevant to lensing) is only marginally affected by the presence of a realistic stellar disc. Disc shocking (e.g. Kazantzidis et al. 2009; D’Onghia et al. 2009) may also reduce the inner substructure abundance, which would further aggravate the problem of explaining the observed lensing anomalies.

In Xu et al. (2009), the dark matter-only Aquarius simulations were used to study the relation between dark matter substructure abundance and lensing flux-ratio anomalies, in particular the cusp-caustic violations observed for multiply imaged quasars. We found that the dark substructures intrinsic to a typical galaxy-scale lensing halo were not sufficient to explain the observed frequency of cusp-caustic violations. In this work, we have considered whether this expectation changes when satellite galaxies in subhaloes are taken into account, or when the lensing halo is assumed to contain a MW-like globular cluster population that is not associated with surviving dark matter substructures. We have also considered streams of dark matter identified in the Aquarius simulations, in order to estimate the lensing effect of irregularities in the halo itself. We conclude that the abundance of intrinsic substructures, dark or bright, bound or diffuse, cannot fully account for the observed cusp-violation frequency. Taken at face value, this lack of substructure suggests a serious problem for the CDM model. Warm dark matter mod-

els, which could reduce the satellite abundance and may help to bring the dwarf galaxy LF into agreement with observations without invoking strong feedback or photoionization effects, (e.g. Sawala et al. 2010) would only make this problem worse. However, it is possible that the observed frequency of flux anomalies are strongly biased by the small number statistics of CLASS.

Previous studies have shown that intergalactic haloes ( $M \lesssim 10^{10} M_\odot$ ) projected along the line of sight can cause surface density fluctuations at the level of 1-10 per cent, making them a probable source of lensing flux anomalies (Chen et al. 2003; Wambsganss et al. 2005; Metcalf 2005a,b; Miranda & Macciò 2007). In future work, we will examine the contribution of this large-scale structure to observations of the cusp-caustic violation rate, using high-resolution cosmological volume simulations, which self-consistently model the halo mass function and clustering along the line of sight (e.g. Puchwein & Hilbert 2009).

## ACKNOWLEDGMENTS

We thank Ian Browne, Neal Jackson and Simon White for useful discussions and the referee for their comments. DDX has been supported by a Dorothy Hodgkin fellowship for her postgraduate studies. LG acknowledges support from a STFC advanced fellowship, one-hundred-talents program of the Chinese Academy of Sciences (CAS) and the National Basic Research Program of China (973 program under grant No. 2009CB24901). CSF acknowledges a Royal Society Wolfson Research Merit award. APC is supported by an STFC postgraduate studentship. The simulations for the Aquarius Project were carried out at the Leibniz Computing Centre, Garching, Germany; at the Computing Centre of the Max Planck Society in Garching; at the Institute for Computational Cosmology in Durham; and on the ‘STELLA’ super-computer of the LOFAR experiment at the University of Groningen.

## REFERENCES

- Amara A., Metcalf R. B., Cox T. J., Ostriker J. P., 2006, MNRAS, 367, 1367
- Anguita T., Faure C., Yonehara A., Wambsganss J., Kneib J.-P., Covone G., Alloin D., 2008, A&A, 481, 615
- Bade N., Siebert J., Lopez S., Voges W., Reimers D., 1997, A&A, 317, L13
- Barnes J., White S. D. M., 1984, MNRAS, 211, 753
- Belokurov V., Evans N. W., Bell E. F., Irwin M. J., Hewett P. C., Koposov S., Rockosi C. M., Gilmore G., Zucker D. B., Fellhauer M., Wilkinson M. I., Bramich D. M., Vidrih S., Rix H., Beers T. C., Schneider D. P., Barentine J. C., Brewington H., 2007, ApJ Letters, 657, L89
- Belokurov V., Evans N. W., Irwin M. J., Lynden-Bell D., Yanny B., Vidrih S., Gilmore G., Seabroke G., Zucker D. B., Wilkinson M. I., Hewett P. C., Bramich D. M., Fellhauer M., Newberg H. J., Wyse R. F. G., Beers T. C., Bell E. F., Barentine J. C., 2007, ApJ, 658, 337
- Benson A. J., Frenk C. S., Lacey C. G., Baugh C. M., Cole S., 2002, MNRAS, 333, 177
- Blandford R., Narayan R., 1986, ApJ, 310, 568



- Blumenthal G. R., Faber S. M., Flores R., Primack J. R., 1986, *ApJ*, 301, 27
- Bower R. G., Benson A. J., Malbon R., Helly J. C., Frenk C., Baugh C., Cole S., Lacey C., 2006, *MNRAS*, 370, 645
- Boylan-Kolchin M., Springel V., White S. D. M., Jenkins A., 2009, *ArXiv e-prints* 0911.4484
- Boylan-Kolchin M., Springel V., White S. D. M., Jenkins A., Lemson G., 2009, *MNRAS*, 398, 1150
- Bradač M., Schneider P., Lombardi M., Steinmetz M., Koopmans L. V. E., Navarro J. F., 2004, *A&A*, 423, 797
- Browne I. W. A., Wilkinson P. N., Jackson N. J. F., Myers S. T., Fassnacht C. D., Koopmans L. V. E., Marlow D. R., Norbury M., Rusin D., Sykes C. M., Biggs A. D., Blandford R. D., de Bruyn A. G., Chae K. H., Helbig P., King L. J., McKean J. P., Pearson T., Phillips P., Readhead A., Xanthopoulos E., York T., 2003, *MNRAS*, 341, 13
- Bryan S. E., Mao S., Kay S. T., 2008, *MNRAS*, 391, 959
- Bullock J. S., Kravtsov A. V., Weinberg D. H., 2000, *ApJ*, 539, 517
- Burud I., Courbin F., Lidman C., Jaunsen A. O., Hjorth J., Ostensen R., Andersen M. I., Clasen J. W., Wucknitz O., Meylan G., Magain P., Stabell R., Refsdal S., 1998, *ApJ Letters*, 501, L5
- Chen J., Kravtsov A. V., Keeton C. R., 2003, *ApJ*, 592, 24
- Chiba M., Minezaki T., Kashikawa N., Kataza H., Inoue K. T., 2005, *ApJ*, 627, 53
- Cole S., Aragon-Salamanca A., Frenk C. S., Navarro J. F., Zepf S. E., 1994, *MNRAS*, 271, 781
- Cole S., Lacey C. G., Baugh C. M., Frenk C. S., 2000, *MNRAS*, 319, 168
- Cooper A. P., Cole S., Frenk C. S., White S. D. M., Helly J., Benson A. J., De Lucia G., Helmi A., Jenkins A., Navarro J. F., Springel V., Wang J., 2010, *MNRAS*, p. 756
- Dalal N., Kochanek C. S., 2002, *ApJ*, 572, 25
- Diemand J., Kuhlen M., Madau P., Zemp M., Moore B., Potter D., Stadel J., 2008, *Nature*, 454, 735
- D'Onghia E., Springel V., Hernquist L., Keres D., 2009, *ArXiv e-prints* 0907.3482
- Efstathiou G., 1992, *MNRAS*, 256, 43P
- Eigenbrod A., Courbin F., Sluse D., Meylan G., Agol E., 2008, *A&A*, 480, 647
- Fassnacht C. D., Blandford R. D., Cohen J. G., Matthews K., Pearson T. J., Readhead A. C. S., Womble D. S., Myers S. T., Browne I. W. A., Jackson N. J., Marlow D. R., Wilkinson P. N., Koopmans L., de Bruyn A., Schilizzi R., Bremer M., Miley G., 1999, *AJ*, 117, 658
- Forte J. C., Martinez R. E., Muzzio J. C., 1982, *AJ*, 87, 1465
- Gao L., De Lucia G., White S. D. M., Jenkins A., 2004, *MNRAS*, 352, L1
- Gao L., Theuns T., Frenk C. S., Jenkins A., Navarro J., Springel V., White S. D. M., 2009, *ArXiv e-prints* 0909.1593
- Gao L., White S. D. M., Jenkins A., Stoehr F., Springel V., 2004, *MNRAS*, 355, 819
- Gavazzi R., Treu T., Rhodes J. D., Koopmans L. V. E., Bolton A. S., Burles S., Massey R. J., Moustakas L. A., 2007, *ApJ*, 667, 176
- Gnedin N. Y., 2000, *ApJ*, 542, 535
- Gnedin O. Y., Kravtsov A. V., Klypin A. A., Nagai D., 2004, *ApJ*, 616, 16
- Griffen B. F., Drinkwater M. J., Thomas P. A., Helly J. C., Pimblett K. A., 2009, *ArXiv e-prints* 0910.0310
- Guo Q., White S., Li C., Boylan-Kolchin M., 2009, *ArXiv e-prints* 0909.4305
- Harris W. E., 1991, *Annual Review of Astronomy and Astrophysics*, 29, 543
- Harris W. E., 1993, in G. H. Smith & J. P. Brodie ed., *The Globular Cluster-Galaxy Connection Vol. 48 of Astronomical Society of the Pacific Conference Series, Photometric Properties of Globular Cluster Systems in Large Galaxies*. p. 472
- Harris W. E., 1996, *AJ*, 112, 1487
- Helly J. C., Cole S., Frenk C. S., Baugh C. M., Benson A., Lacey C., 2003, *MNRAS*, 338, 903
- Helmi A., White S. D. M., 1999, *MNRAS*, 307, 495
- Impey C. D., Foltz C. B., Petry C. E., Browne I. W. A., Patnaik A. R., 1996, *ApJ Letters*, 462, L53
- Jackson N., Bryan S. E., Mao S., Li C., 2010, *MNRAS*, 403, 826
- Jackson N., Nair S., Browne I. W. A., Wilkinson P. N., Muxlow T. W. B., de Bruyn A. G., Koopmans L., Bremer M., Snellen I., Miley G. K., Schilizzi R. T., Myers S., Fassnacht C. D., Womble D. S., Readhead A. C. S., Blandford R. D., Pearson T. J., 1998, *MNRAS*, 296, 483
- Jackson N., Xanthopoulos E., Browne I. W. A., 2000, *MNRAS*, 311, 389
- Kauffmann G., White S. D. M., Guiderdoni B., 1993, *MNRAS*, 264, 201
- Kazantzidis S., Zentner A. R., Kravtsov A. V., Bullock J. S., Debattista V. P., 2009, *ApJ*, 700, 1896
- Keeton C. R., Gaudi B. S., Petters A. O., 2003, *ApJ*, 598, 138
- Klypin A., Kravtsov A. V., Valenzuela O., Prada F., 1999, *ApJ*, 522, 82
- Kochanek C. S., Dalal N., 2004, *ApJ*, 610, 69
- Koopmans L. V. E., Treu T., Bolton A. S., Burles S., Moustakas L. A., 2006, *ApJ*, 649, 599
- Koposov S., Belokurov V., Evans N. W., Hewett P. C., Irwin M. J., Gilmore G., Zucker D. B., Rix H.-W., Fellhauer M., Bell E. F., Glushkova E. V., 2008, *ApJ*, 686, 279
- Kravtsov A., 2010, *Advances in Astronomy*, 2010
- Li G. L., Mao S., Jing Y. P., Kang X., Bartelmann M., 2006, *ApJ*, 652, 43
- Li Y.-S., De Lucia G., Helmi A., 2010, *MNRAS*, 401, 2036
- Macciò A. V., Kang X., Moore B., 2009, *ApJ Letters*, 692, L109
- Macciò A. V., Miranda M., 2006, *MNRAS*, 368, 599
- Macciò A. V., Moore B., Stadel J., Diemand J., 2006, *MNRAS*, 366, 1529
- MacLeod C. L., Kochanek C. S., Agol E., 2009, *ApJ*, 699, 1578
- Mao S., Jing Y., Ostriker J. P., Weller J., 2004, *ApJ Letters*, 604, L5
- Mao S., Schneider P., 1998, *MNRAS*, 295, 587
- Maraston C., 2005, *MNRAS*, 362, 799
- McConnachie A. W., Irwin M. J., Ibata R. A., Dubinski J., Widrow L. M., Martin N. F., Côté P., Dotter A. L., Navarro J. F., Ferguson A. M. N., Puzia T. H., Lewis G. F., Babul A., Barmby P., Bienaymé O., 2009, *Nature*, 461, 66
- McKean J. P., Koopmans L. V. E., Flack C. E., Fassnacht C. D., Thompson D., Matthews K., Blandford R. D.,

- Readhead A. C. S., Soifer B. T., 2007, MNRAS, 378, 109
- Metcalf R. B., 2005a, ApJ, 622, 72
- Metcalf R. B., 2005b, ApJ, 629, 673
- Metcalf R. B., Madau P., 2001, ApJ, 563, 9
- Metcalf R. B., Moustakas L. A., Bunker A. J., Parry I. R., 2004, ApJ, 607, 43
- Metcalf R. B., Zhao H., 2002, ApJ Letters, 567, L5
- Miranda M., Macciò A. V., 2007, MNRAS, 382, 1225
- Mo H. J., Mao S., White S. D. M., 1998, MNRAS, 295, 319
- Moore B., Ghigna S., Governato F., Lake G., Quinn T., Stadel J., Tozzi P., 1999, ApJ Letters, 524, L19
- More A., McKean J. P., More S., Porcas R. W., Koopmans L. V. E., Garrett M. A., 2009, MNRAS, 394, 174
- Morgan N. D., Kochanek C. S., Falco E. E., Dai X., 2006, in Bulletin of the American Astronomical Society Vol. 38, Time-Delays and Mass Models for the Quadruple Lens RXJ1131-1231. p. 927
- Myers S. T., Jackson N. J., Browne I. W. A., de Bruyn A. G., Pearson T. J., Readhead A. C. S., Wilkinson P. N., Biggs A. D., Blandford R. D., Fassnacht C. D., Koopmans L. V. E., Marlow D. R., McKean J. P., Norbury M. A., Phillips P. M., Rusin D., Shepherd M. C., Sykes C. M., 2003, MNRAS, 341, 1
- Navarro J. F., Ludlow A., Springel V., Wang J., Vogelsberger M., White S. D. M., Jenkins A., Frenk C. S., Helmi A., 2010, MNRAS, 402, 21
- Okamoto T., Frenk C. S., 2009, MNRAS, 399, L174
- Patnaik A. R., Narasimha D., 2001, MNRAS, 326, 1403
- Peñarrubia J., Navarro J. F., McConnachie A. W., 2008, ApJ, 673, 226
- Pooley D., Blackburne J. A., Rappaport S., Schechter P. L., 2007, ApJ, 661, 19
- Puchwein E., Hilbert S., 2009, MNRAS, 398, 1298
- Rusin D., Kochanek C. S., 2005, ApJ, 623, 666
- Rusin D., Kochanek C. S., Keeton C. R., 2003, ApJ, 595, 29
- Sawala T., Guo Q., Scannapieco C., Jenkins A., White S. D. M., 2010, ArXiv e-prints 1003.0671
- Schneider P., Weiss A., 1992, A&A, 260, 1
- Sluse D., Surdej J., Claeskens J.-F., Hutsemékers D., Jean C., Courbin F., Nakos T., Billeres M., Khmil S. V., 2003, A&A, 406, L43
- Springel V., Wang J., Vogelsberger M., Ludlow A., Jenkins A., Helmi A., Navarro J. F., Frenk C. S., White S. D. M., 2008, MNRAS, 391, 1685
- Springel V., White S. D. M., Frenk C. S., Navarro J. F., Jenkins A., Vogelsberger M., Wang J., Ludlow A., Helmi A., 2008, Nature, 456, 73
- Strigari L. E., Bullock J. S., Kaplinghat M., Simon J., Geha M., Willman B., Walker M., 2008, Nature, 454, 1096
- Stringer M., Cole S., Frenk C., 2009, ArXiv e-prints 0911.1888
- Sugai H., Kawai A., Shimono A., Hattori T., Kosugi G., Kashikawa N., Inoue K., Chiba M., 2007, ApJ, 660, 1016
- Tollerud E. J., Bullock J. S., Strigari L. E., Willman B., 2008, ApJ, 688, 277
- Turner E. L., Ostriker J. P., Gott III J., 1984, ApJ, 284, 1
- Vegetti S., Koopmans L. V. E., 2009, MNRAS, p. 1456
- Vegetti S., Koopmans L. V. E., Bolton A., Treu T., Gavazzi R., 2009, ArXiv e-prints 0910.0760
- Wambsganss J., Bode P., Ostriker J. P., 2005, ApJ Letters, 635, L1
- Wambsganss J., Paczynski B., Schneider P., 1990, ApJ Letters, 358, L33
- West M. J., 1993, MNRAS, 265, 755
- White S. D. M., Rees M. J., 1978, MNRAS, 183, 341
- Witt H. J., Mao S., Schechter P. L., 1995, ApJ, 443, 18
- Xu D. D., Mao S., Wang J., Springel V., Gao L., White S. D. M., Frenk C. S., Jenkins A., Li G., Navarro J. F., 2009, MNRAS, 398, 1235
- Zakharov A. F., 1995, A&A, 293, 1